HIGH TEMPERATURE PROTONIC CONDUCTORS

Fred Dynys[1], Marie-Helene Berger[2], & Ali Sayir[3]
1 NASA-GRC, 21000 Brookpark Rd., Cleveland, OH 44135, USA
2 Ecole des Mines de Paris – Centre des Matériaux BP 87 – 91003 Evry cedex – France
3 CWRU, 10900 Euclid Ave, Cleveland, OH 44112, USA

High Temperature Protonic Conductors (HTPC) with the perovskite structure are envisioned for electrochemical membrane applications such as H_2 separation, H_2 sensors and fuel cells. Successive membrane commercialization is dependent upon addressing issues with H_2 permeation rate and environmental stability with CO_2 and H_2O. HTPC membranes are conventionally fabricated by solid-state sintering. Grain boundaries and the presence of intergranular second phases reduce the proton mobility by orders of magnitude than the bulk crystalline grain. To enhanced protonic mobility, alternative processing routes were evaluated. A laser melt modulation (LMM) process was utilized to fabricate bulk samples, while pulsed laser deposition (PLD) was utilized to fabricate thin film membranes .

$Sr_3Ca_{1+x}Nb_{2-x}O_9$ and $SrCe_{1-x}Y_xO_3$ bulk samples were fabricated by LMM. Thin film $BaCe_{0.85}Y_{0.15}O_3$ membranes were fabricated by PLD on porous substrates. Electron microscopy with chemical mapping was done to characterize the resultant microstructures. High temperature protonic conduction was measured by impedance spectroscopy in wet air or H_2 environments. The results demonstrate the advantage of thin film membranes to thick membranes but also reveal the negative impact of defects or nanoscale domains on protonic conductivity.

High Temperature Protonic Conductors

F.W. Dynys
NASA-Glenn Research Center

M. H. Berger
Ecole des Mines de Paris

A.Sayir
CWRU/NASA-Glenn Research Center

Sponsors: NASA Glenn Research Center Internal Research and Development Program.

European Office of Aerospace Research & Development by AFOSR under Grant # FA8655-03-1-3040.

Outline

A. Introduction

B. Sintering

- $BaCe_{0.85}Y_{0.15}O_{3-\delta}$

C. Directional Solidification

- $SrCe_{0.9}Y_{0.1}O_{3-\delta}$
- $Sr_3Ca_{1.18}Nb_{1.82}O_{9-\delta}$

C. Thin Film Deposition

- $BaCe_{0.85}Y_{0.15}O_{3-\delta}$

D. Summary

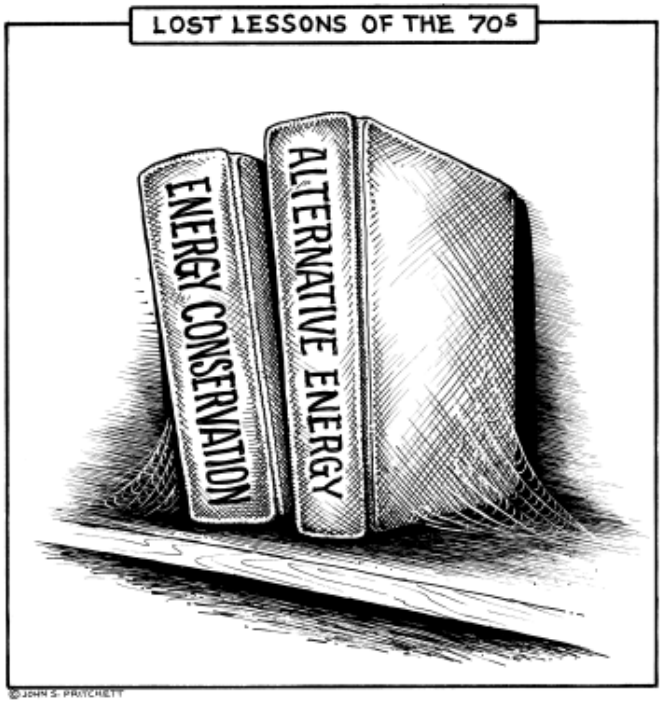

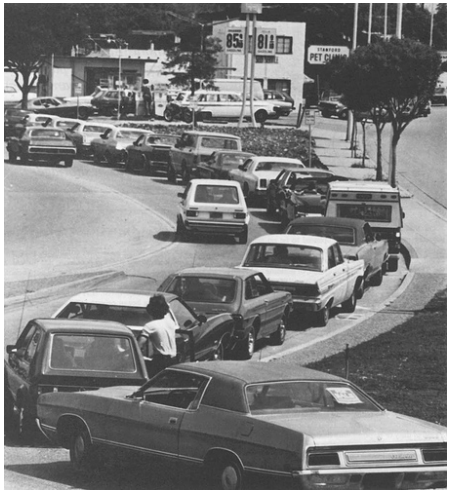

World Energy Demand Growing Dramatically

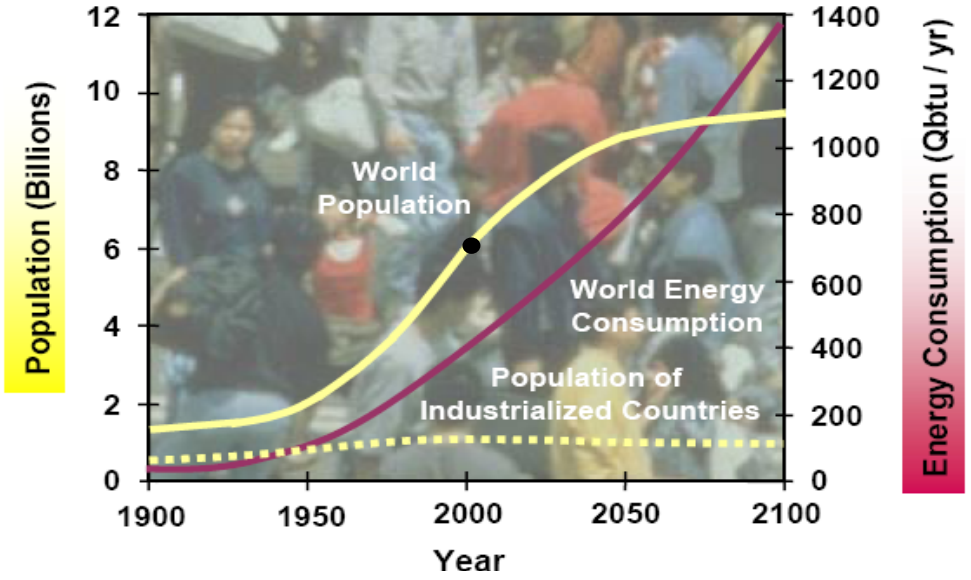

Challenges

- **Renewable energy supply will be essential:** Wind, Solar, Bio-fuels Geothermal & Solar thermal
- **New forms of energy are vital:** H_2
- **New sources:** Methane hydrates
- **Improve efficiency:** Extend finite resources
- **Technology:** Drive energy cost reduction

Functional Oxide Materials for Energy Applications

Oxide ceramics – Electrochemical properties

- Oxygen transport – selectivity >1000
- H_2 transport – selectivity >1000

Applications

- Sensors - CO, CO_2, H_2, NO_x detection
- Power - Solid oxide fuel cells
- Electrolyzers
- Membrane reactors – chemical processing

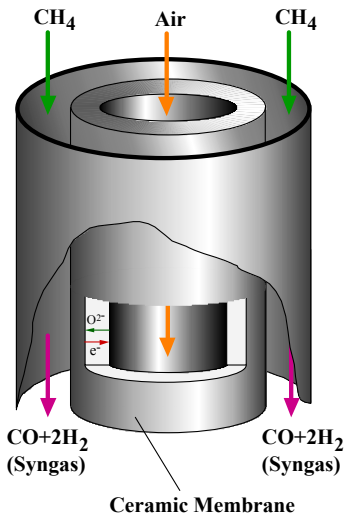

$CH_4 + {}^1/_2O_2 \rightarrow CO + 2H_2$

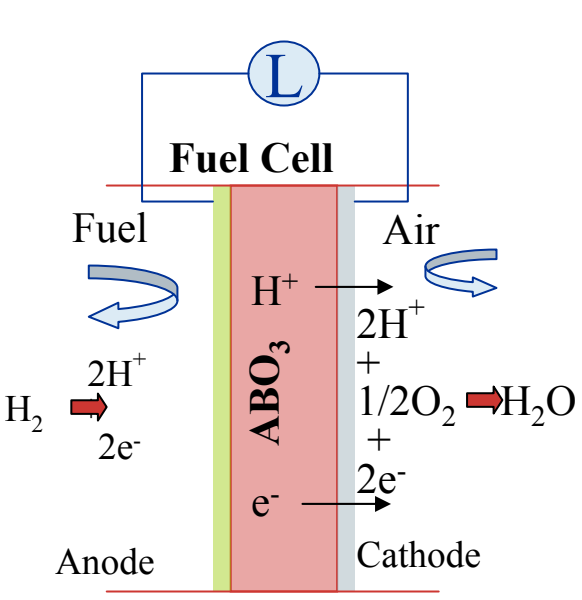

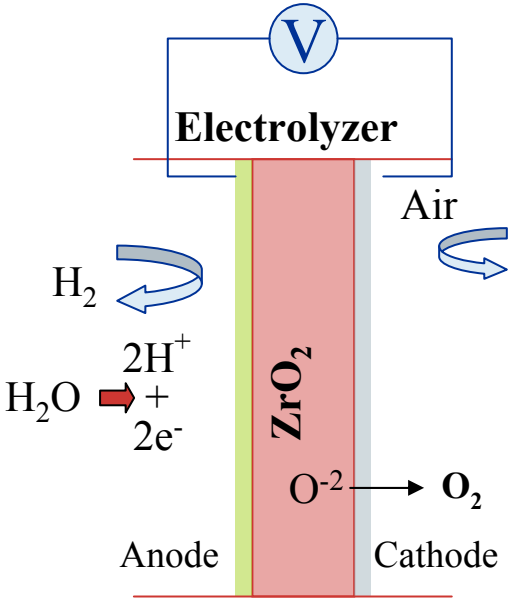

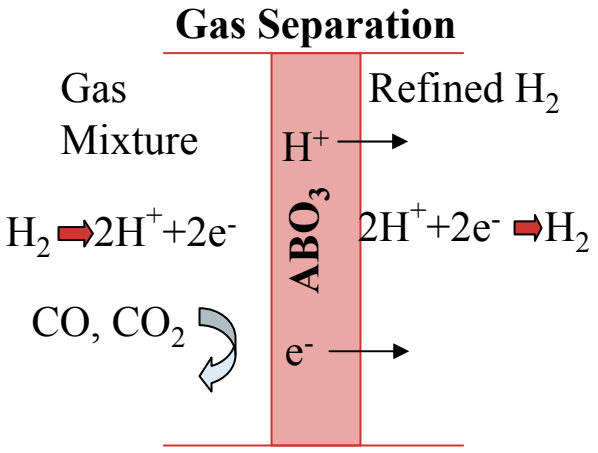

High Temperature Protonic Ceramics

Crystal Structures: Perovskite - ABO_3, $A_2(B'B'')O_{6-\delta}$ & $A_3(B'B_2'')O_{9-\delta}$

Fluorite – M_2O_3

Pyrochlore – $A_2B_2O_7$

ABO_3 – $Pm\bar{3}m$

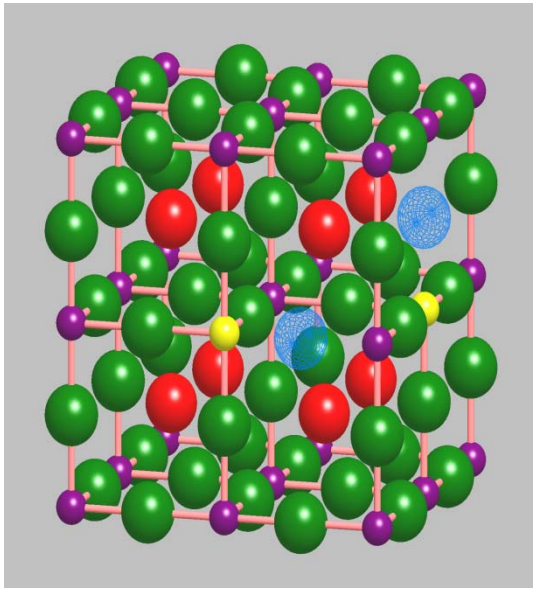

Proton Insertion

Oxygen vacancies ($V_O^{\bullet\bullet}$) needed for H^+ transport:

B site doping: $2B_B + O_O + M_2O_3 \longrightarrow 2M_{Ce} + V_O^{\bullet\bullet} + 2BO_2$

Humid environment: $H_2O_{(g)} + V_O^{\bullet\bullet} + O_O \longrightarrow 2OH_O^{\bullet}$

H_2 environment: $V_O^{\bullet\bullet} + 1/2O_2 \longrightarrow O_O + 2h^{\bullet}$

$H_{2(g)} + 2O_O + 2h^{\bullet} \longrightarrow 2OH_O^{\bullet}$

Proton strongly associates with a neighbouring oxygen ion-represented as OH

Distorted Perovskite Structure

$$\text{tolerance factor} = \frac{R_A + R_O}{\sqrt{2} \bullet (R_B + R_O)}$$

t<0.96 tetragonal/orthorhombic

Cubic → Non-Cubic

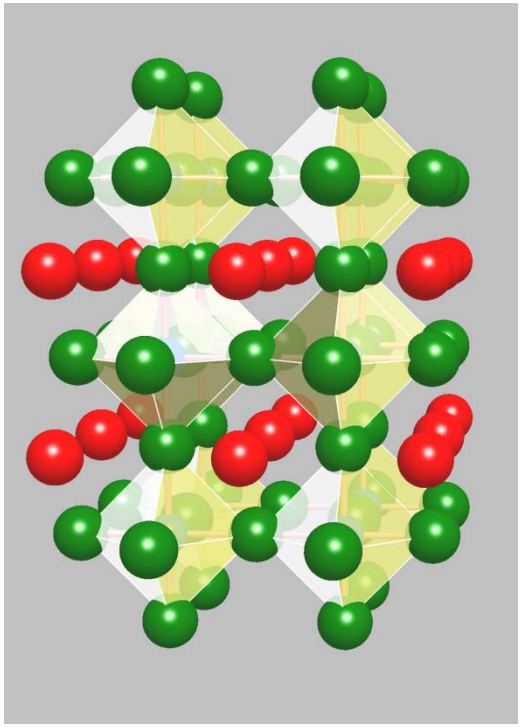

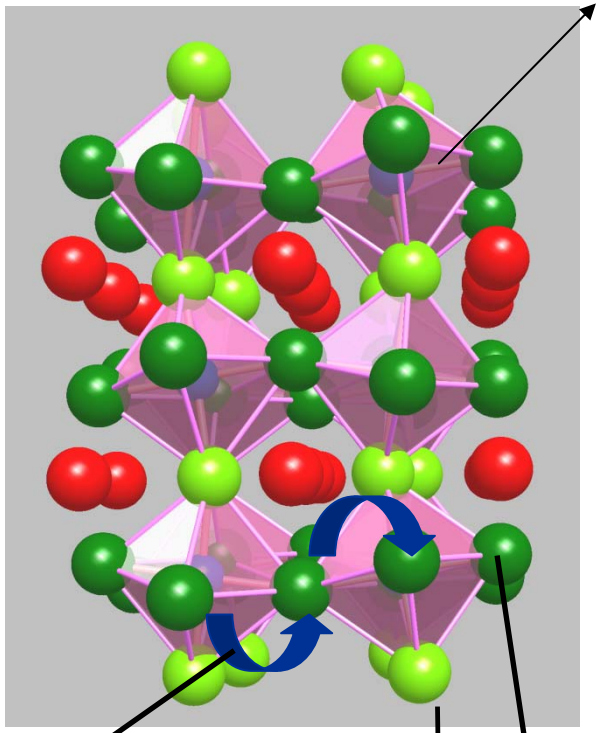

Octahedra Tilting

- BO_6 octahedra tilt to reduce A site volume
- $SrCeO_3$ 11°& 12.5°
- $BaCeO_3$ 6° & 8.8°

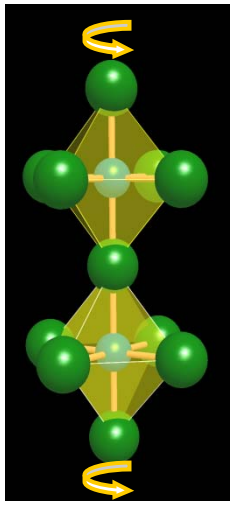

In-phase

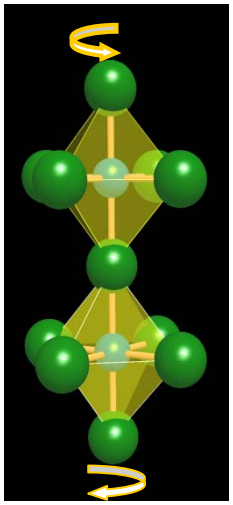

Antiphase

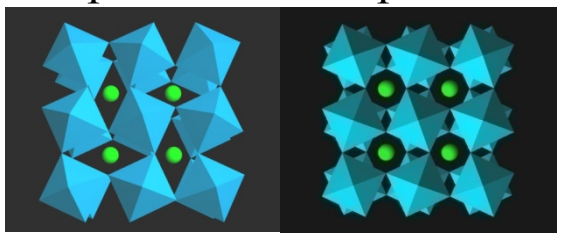

Predominant proton transfer path

Independent Oxygen sites

O1 O2

Protonic Ceramic Development

Ceramic

Optimization of Composition
$(A_xA_{1-x})(B_yB_{1-y})O_{3-\delta}$

Solid State Sintering

Multiphase Materials
Maximize σ
Ionic/Electronic

Cermets

Thin Film Structures
Maximize
Permeation Rate

Opportunities

Argonne National Laboratory

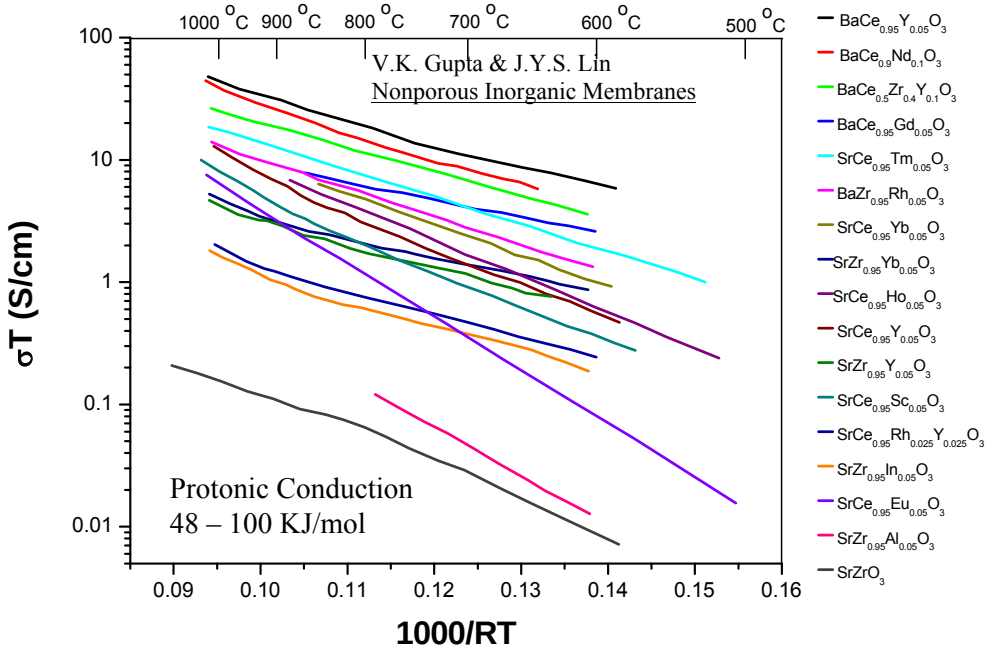

A-Site Doping
- Proton Uptake
- Chemical Stability
- Mechanical Stability

B-Site Doping
- O_2 Vacancies
- Proton mobility
- Electron σ
- Proton Uptake
- Chemical Stability
- Mechanical Stability

Basic Science
- Crystal Structure
- Thermodynamics

Grain Boundary
- Detrimental to H^+ transport

Environmental
- Reactive CO_2
- Reactive H_2O

Impedance Spectroscopy

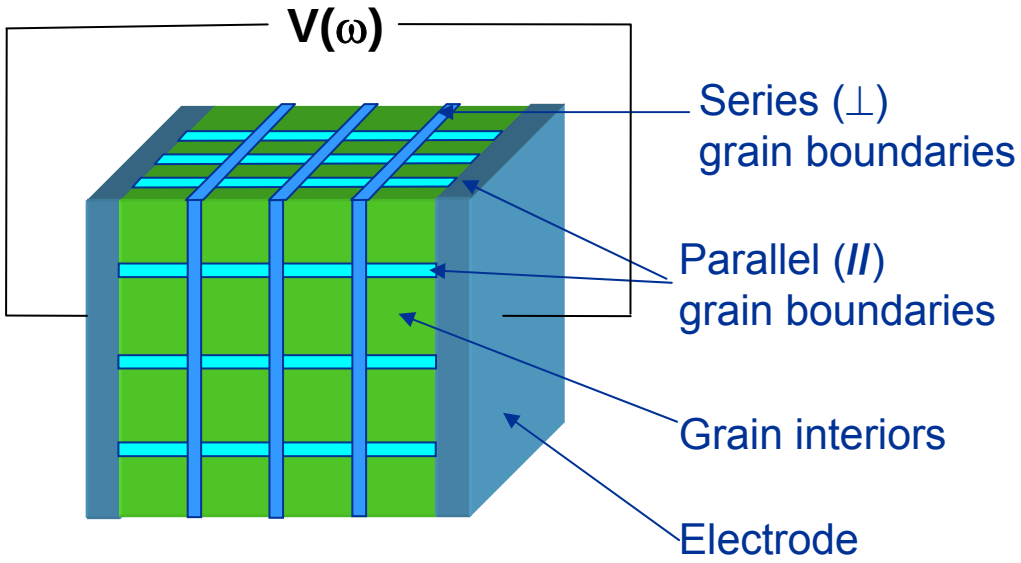

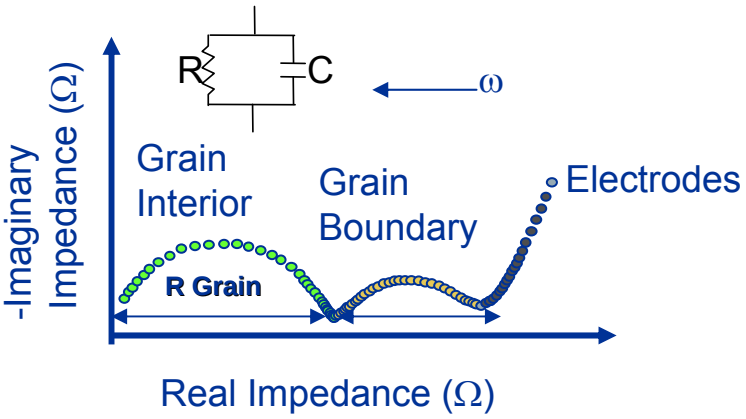

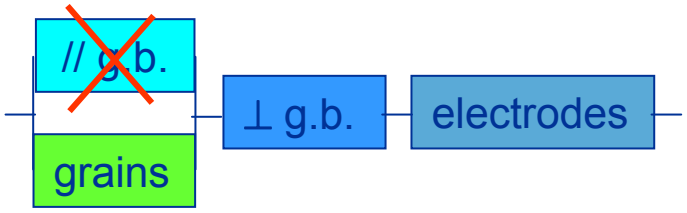

conduction: grain ≠ grain boundary

ω_0 grain boundary << ω_0 grain-Low T

ω_0 grain boundary ~ ω_0 grain-High T

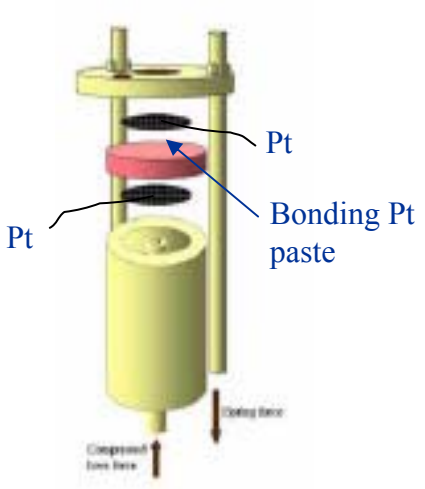

Experimental Set-Up

Sintering Protonic Ceramics

$BaCe_{0.85}Y_{0.15}O_{3-\delta}$

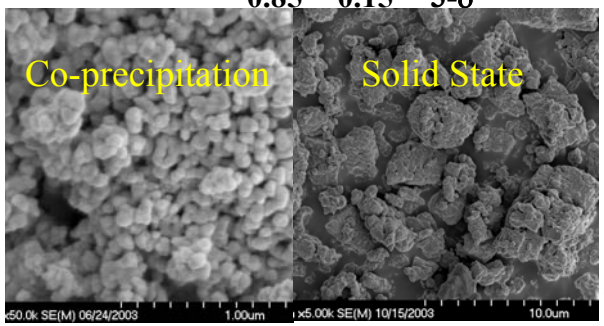

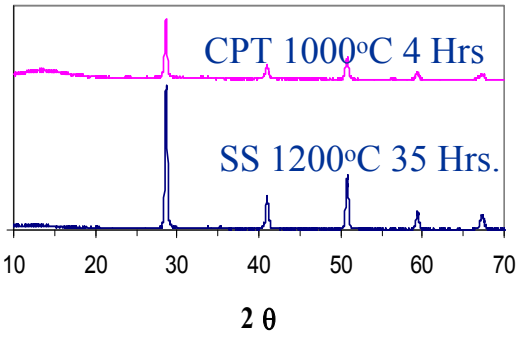

1650 °C 10 Hrs.

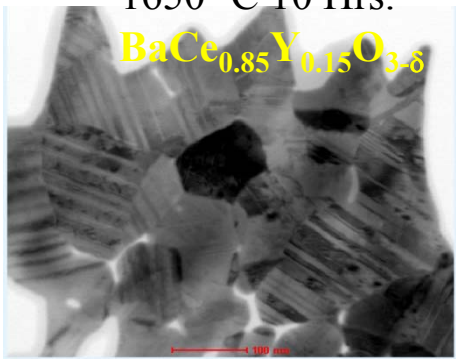

High Sintering Temp.

Composition	T °C	% ρ	Composition	T °C	% ρ
$BaZr_{1-x}Y_xO_{3-\delta}$ x=0.02-0.25	1700	87 - 95	$SrTi_{1-x}Sc_xO_{3-\delta}$, x=0.02-0.05	1590	80 - 90
$BaZr_{0.9}Sc_{0.1}O_{3-\delta}$	1700	91	$Sr_{0.66}Ba_{0.33}Ti_{0.95}Sc_{0.05}O_{3-\delta}$	1560	90
$BaZr_{0.9}In_{0.1}O_{3-\delta}$	1700	93	$Sr_{0.33}Ba_{0.66}Zr_{0.56}Y_{0.1}Ti_{0.33}O_{3-\delta}$	1600	93
$BaZr_{0.9}Gd_{0.1}O_{3-\delta}$	1650	88	$Sr_{0.66}Ba_{0.33}Zr_{0.33}Sc_{0.05}Ti_{0.61}O_{3-\delta}$	1650	88
$Ba_{0.66}Sr_{0.33}Zr_{0.9}Y_{0.1}O_{3-\delta}$	1630	88	$SrZr_{0.33}Sc_{0.05}Ti_{0.61}O_{3-\delta}$	1590	94
$SrZr_{0.9}Y_{0.1}O_{3-\delta}$	1675	94	$BaZr_{0.45}Y_{0.1}Ti_{0.45}O_{3-\delta}$	1600	87
$SrHf_{0.9}Y_{0.1}O_{3-\delta}$	1600	82			

Kreuer et al.,Solid State Ionics 145 2001 295–306

$BaY_{0.1}Ce_{0.9}O_{3-\delta}$

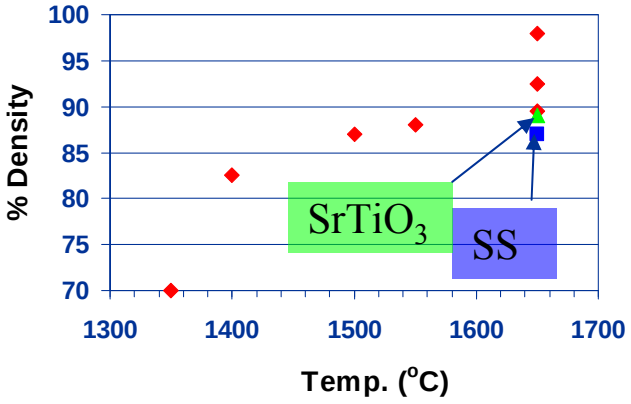

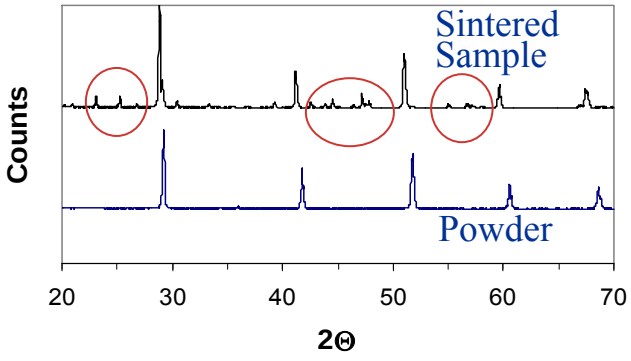

Directional Solidification

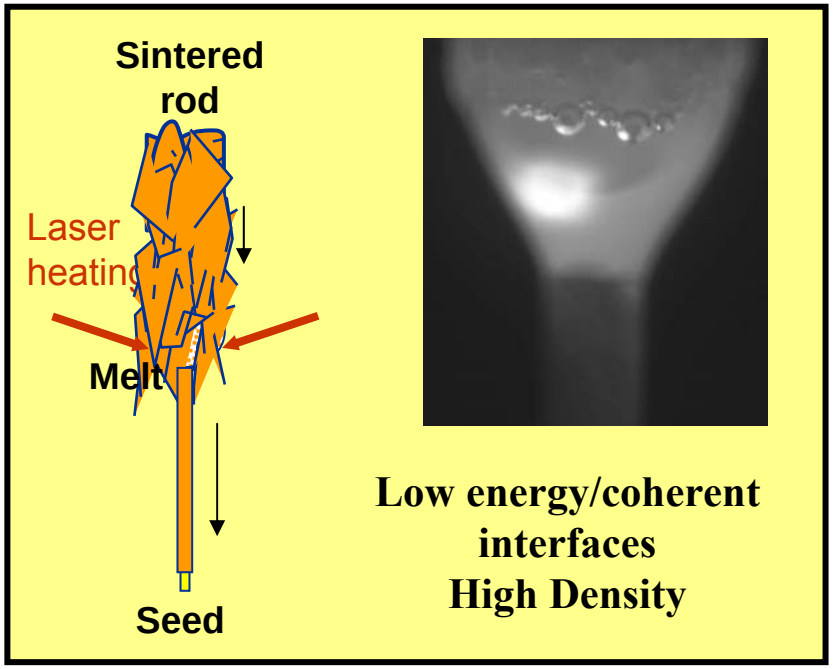

Microstructure-$SrCe_{0.9}Y_{0.1}O_{3-\delta}$ - Chemistry

Textured Microstructure

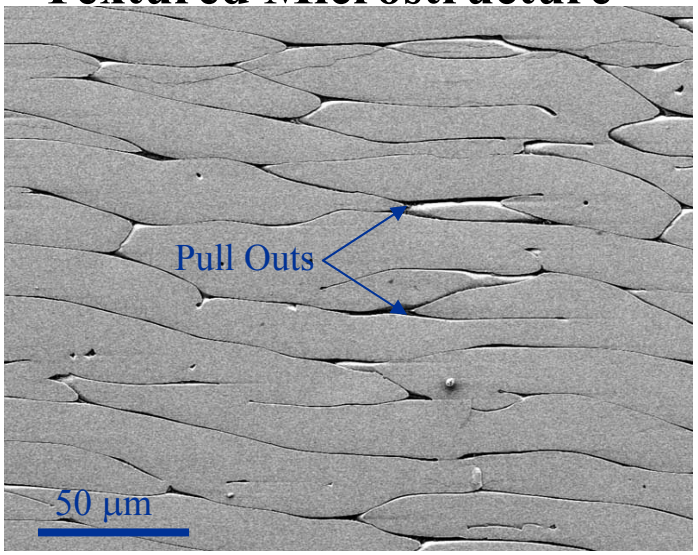

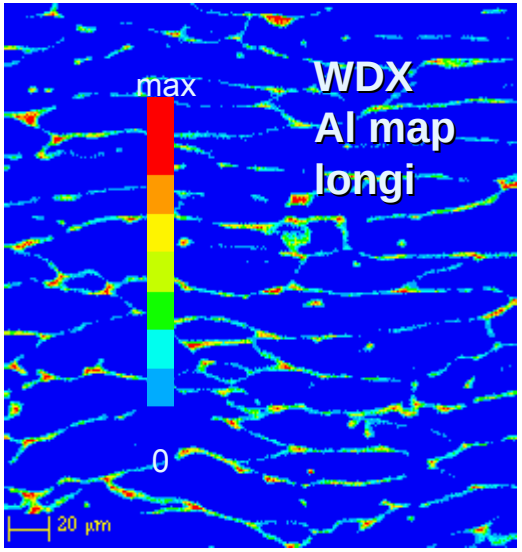

- Al 2nd phase contaminant – conc. between grains

  Pre-fabrication contamination

Microstructure - $Sr_3(Ca_{1+x}Nb_{2-x})O_{9-\delta}$ - Chemistry

Dense - Cellular growth

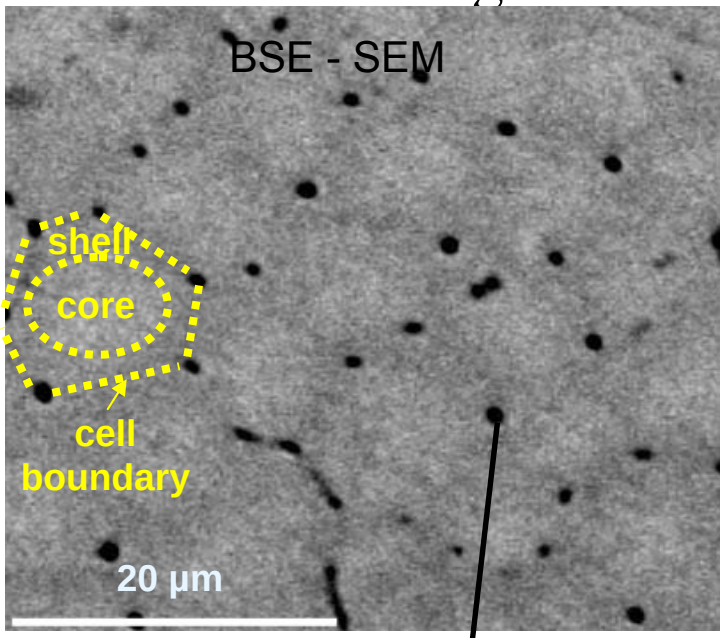

Core : Ca^{2+}, Sr^{2+} rich

Shell : Nb^{5+}, O^{2-} rich

2nd phases : Sr^{2+}, O^{2-} rich

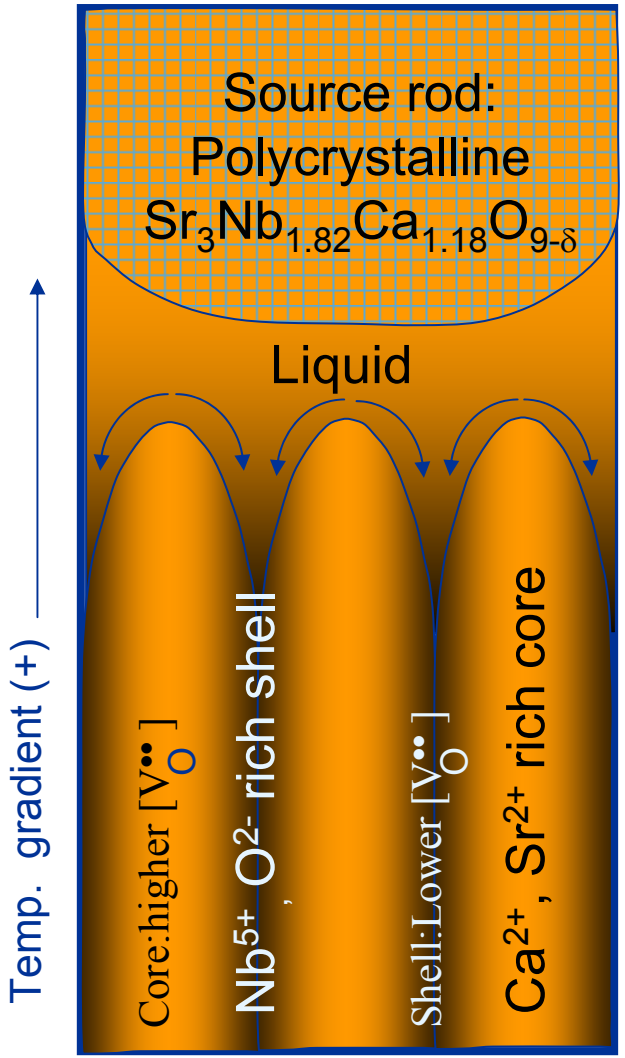

WDX maps

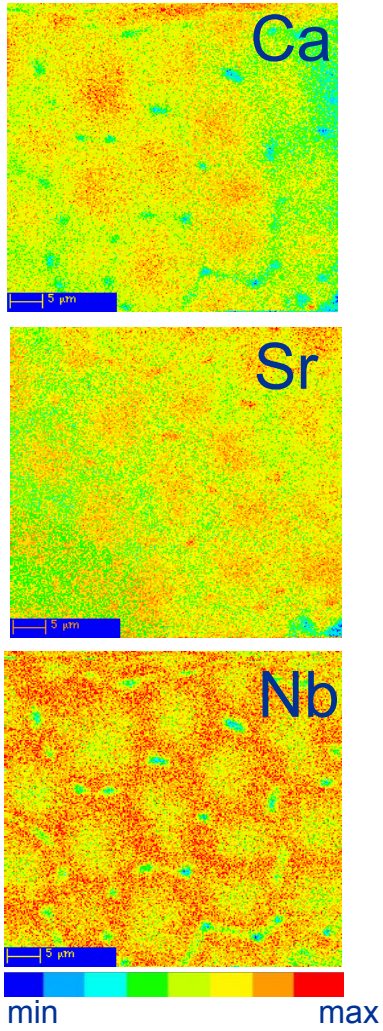

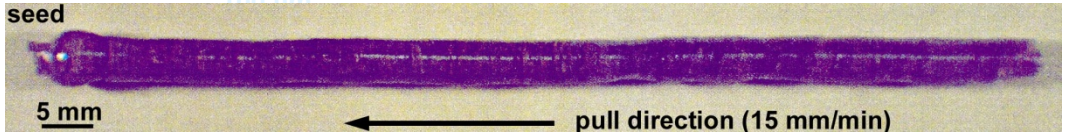

$SrCe_{0.9}Y_{0.1}O_{3-\delta}$

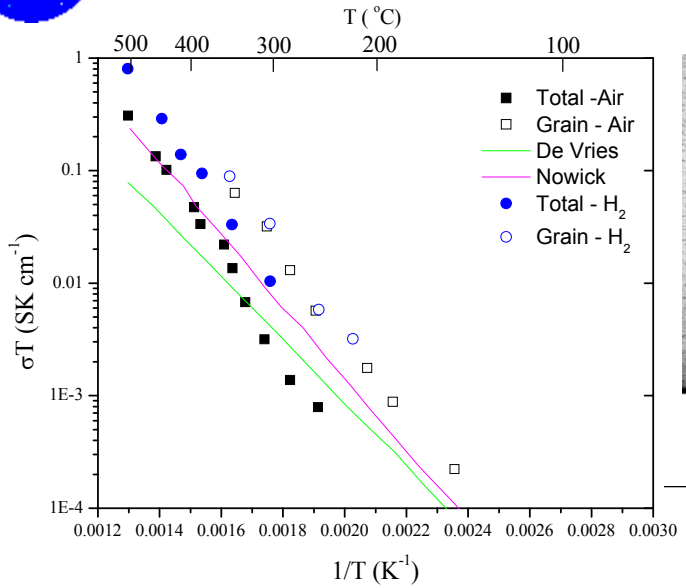

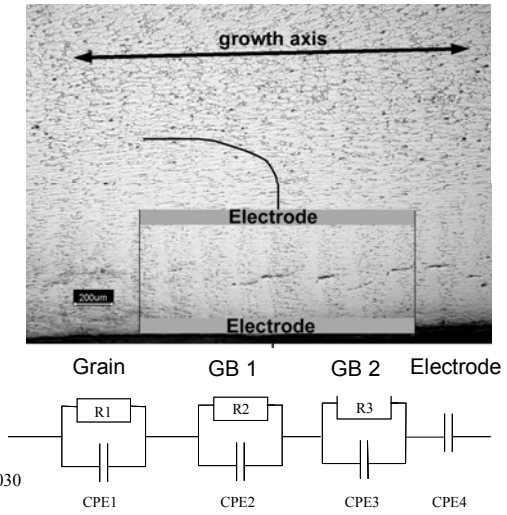

Equivalent Circuit

$$\sigma \cdot T = A \cdot \exp(-Q/RT)$$

Activation Energy

Total σ	Q (KJ/mol)
$SrCa_{0.9}Y_{0.1}O_{3-\delta}$ Air H_2	83.2 98.1
De Vries	53.6
Nowick	60.8

$Sr_3(Ca_{1+x}Nb_{2-x})O_{9-\delta}$

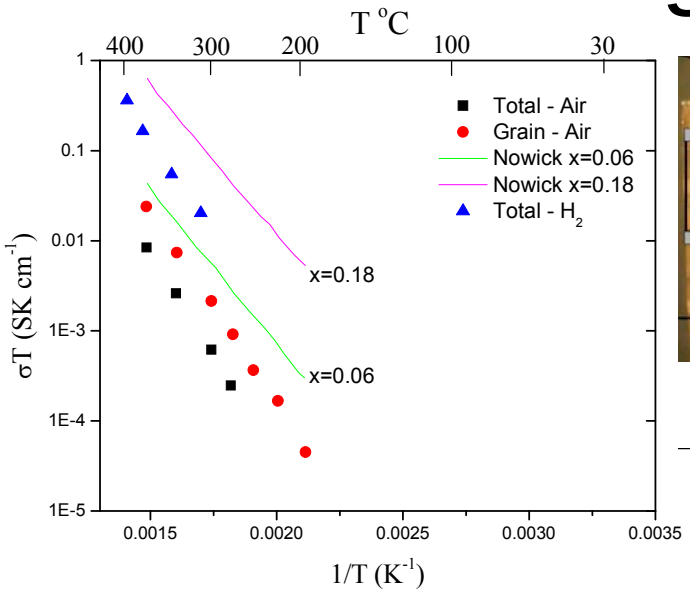

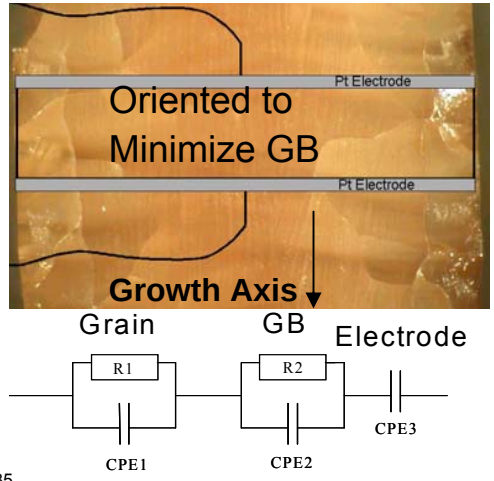

Equivalent Circuit

Activation Energy

Total σ	Q (KJ/mol)
$Sr_3Ca_{1.18}Nb_{1.82}O_{9-}$ Air H_2	84.6 98.1
Nowick $Sr_3Ca_{1.06}Nb_{1.94}O_{9-\delta}$	66.5
Nowick $Sr_3Ca_{1.18}Nb_{1.82}O_{9-\delta}$	63.6

Protonic Conduction
48 – 100 KJ/mol

Nano-Structure Domains

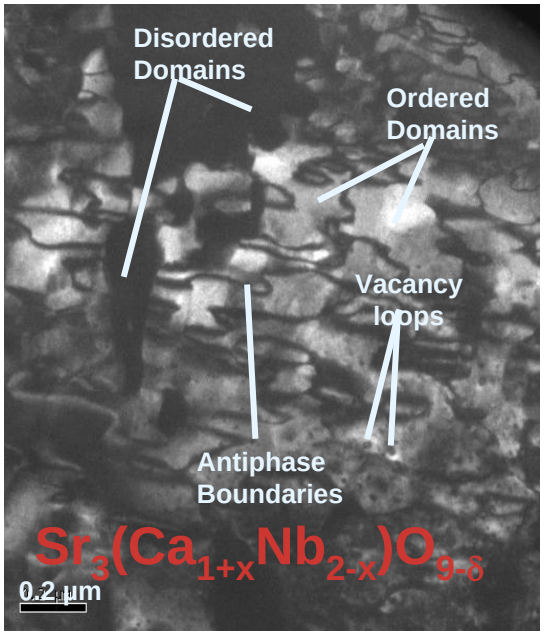

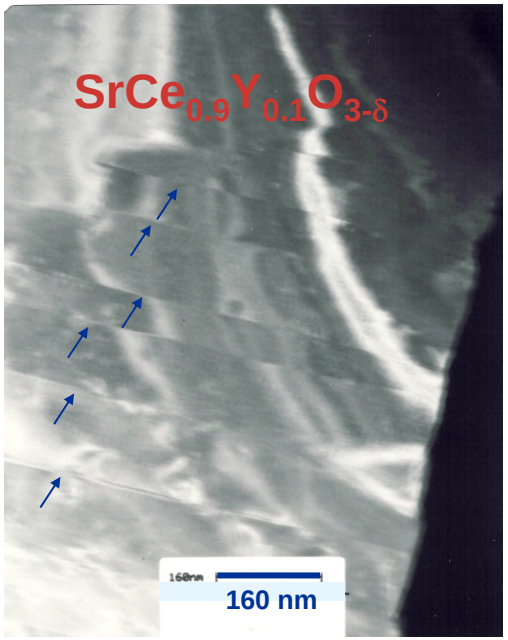

1650 °C 10 Hrs.

Nanostructures → Protonic transport ?

Thin Film Electrolytes

Thickness Dependence

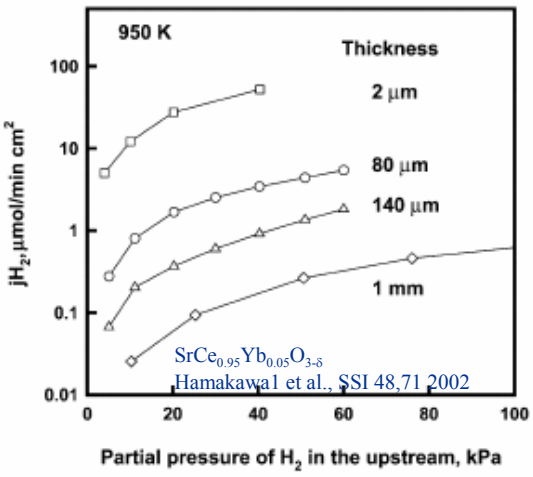

$SrCe_{0.95}Yb_{0.05}O_{3-\delta}$
Hamakawa1 et al., SSI 48,71 2002

GS Dependence

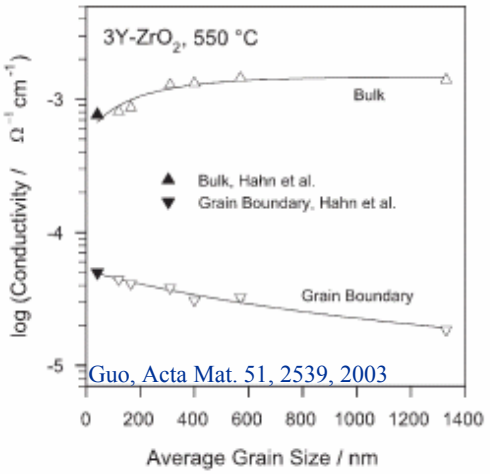

Guo, Acta Mat. 51, 2539, 2003

Supported electrolyte fabrication difficult with high sintering temp.

PVD Microstructure

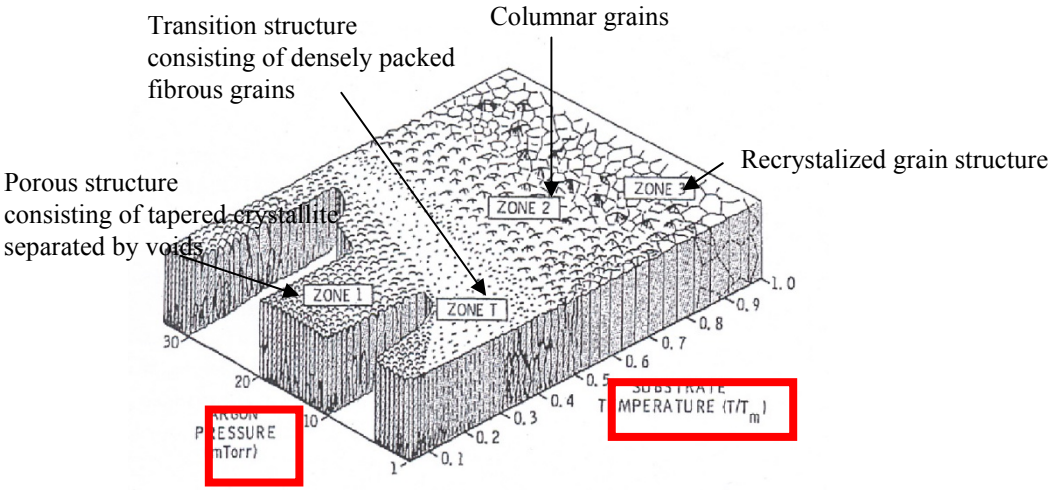

Approach

Pulsed Laser Deposition

- Stoichiometry
- Simple
- High Energy
- High Depostion Rate

Pulsed Laser Deposition

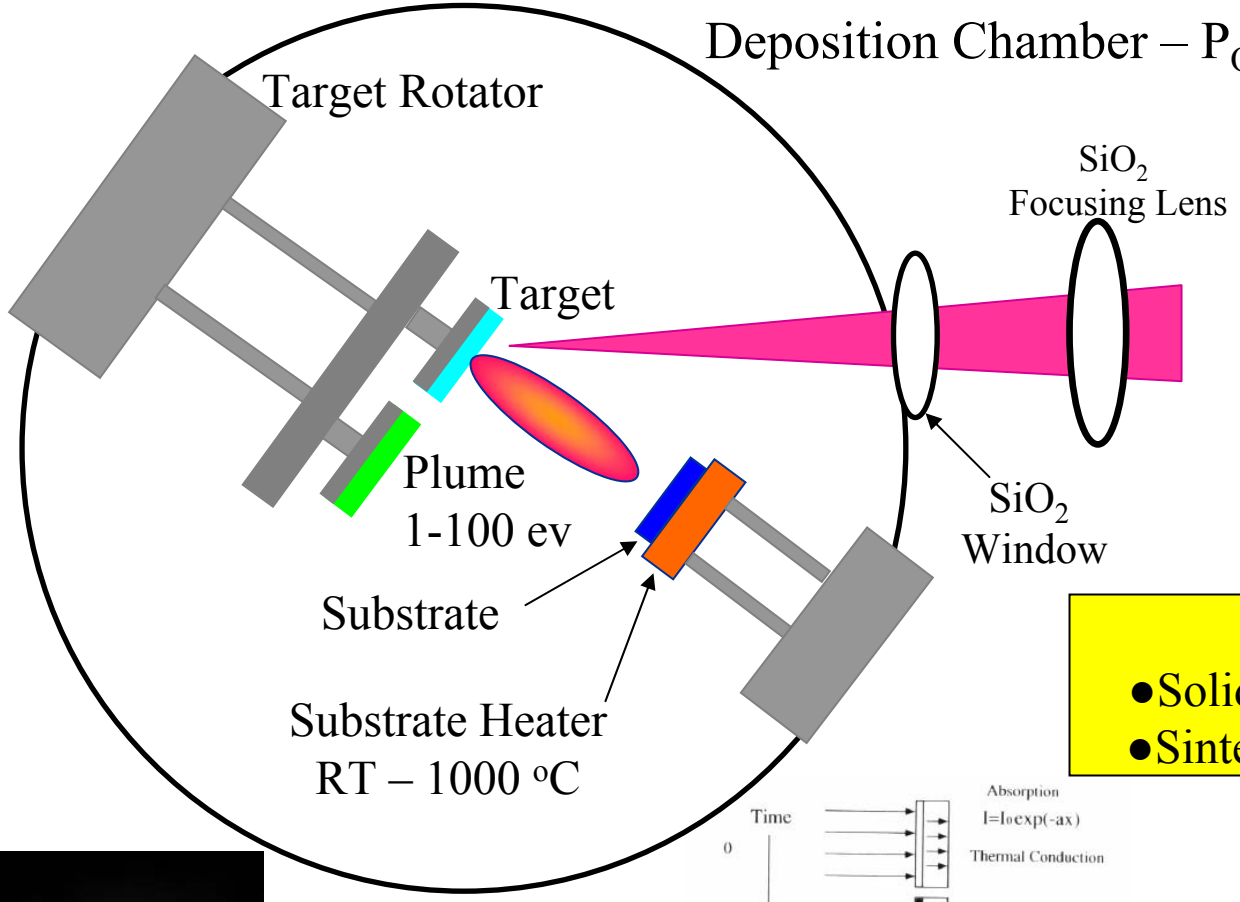

Excimer Laser

- λ = 248 nm -KrF
- Energy: 1 – 3 J/cm^2
- Frequency: <10 Hz
- Pulse: 25 ns

Targets

- Solid state synthesize powder
- Sintering – 1650 °C 10 hrs. air

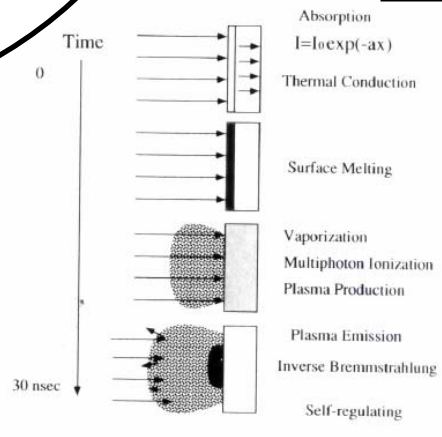

Substrates

- Porous Al_2O_3
- Porous $BaZrO_3$
- Silicon

Silicon Substrates

$BaCe_{0.85}Y_{0.15}O_{3-\delta}$

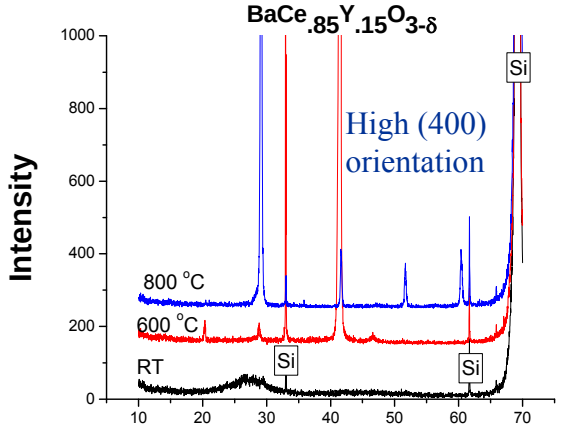

700 °C

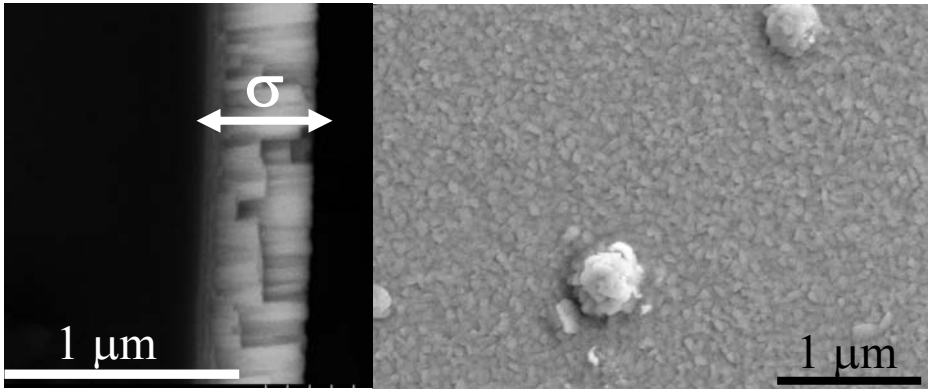

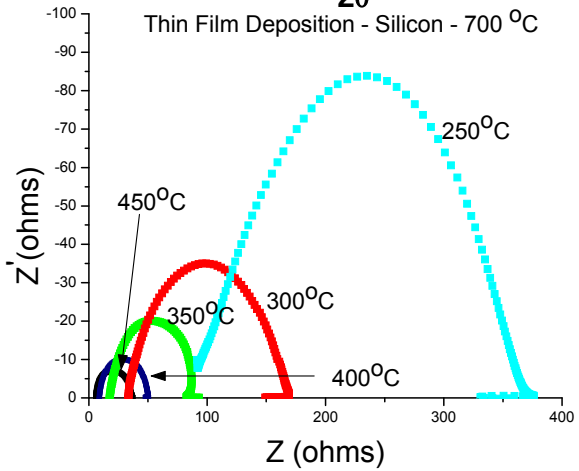

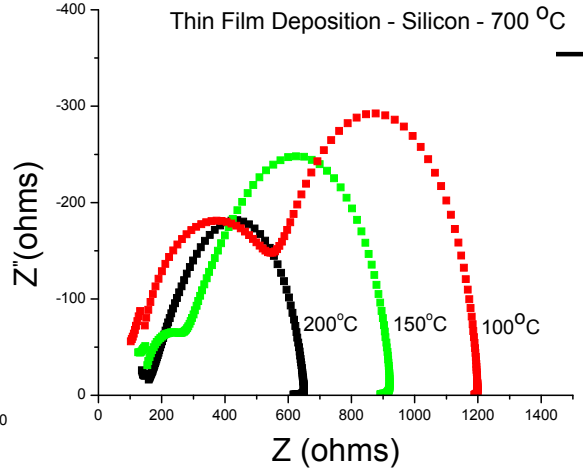

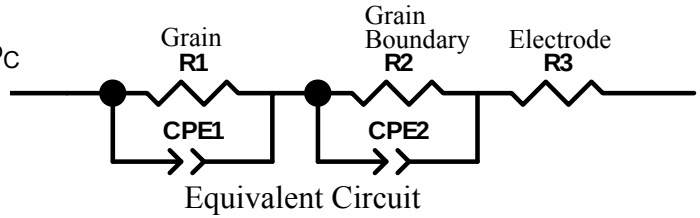

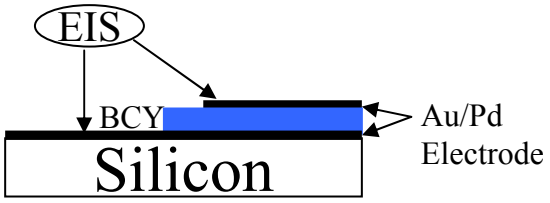

Solartron 1260/1287 0.1 – 1MHz 100 °C – 500 °C
Moist Argon – 25 °C Zplot/Zview Software

Total Conductivity
Silicon Substrates

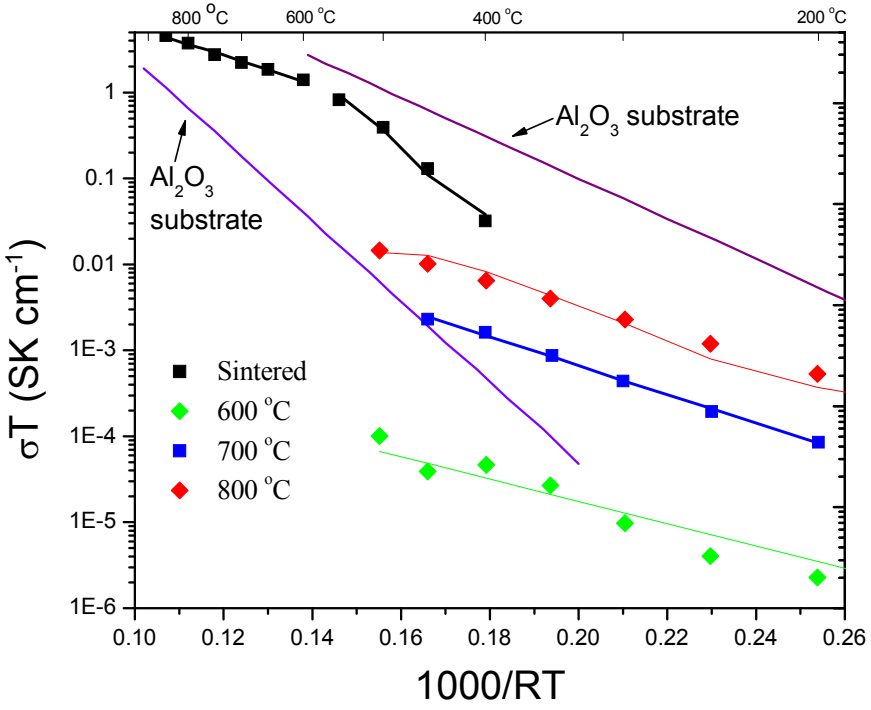

$$\sigma \cdot T = A \cdot \exp(-Q/RT)$$

Activation Energy

	Temp. (°C)	Q (KJ/mol)	Film Thickness (μm)
$BaCe_{0.85}Y_{0.15}O_3$ Sintered	600 - 850 400 - 550	38.6 100.3	
800 °C/30 mT	100 - 500	33.4	6
700 °C/30 mT	200 – 500	38.2	6
600 °C/30 mT	100 – 500	29.9	2.4

Protonic Conduction – 48 – 100 KJ/mol

Porous Al_2O_3 Substrates

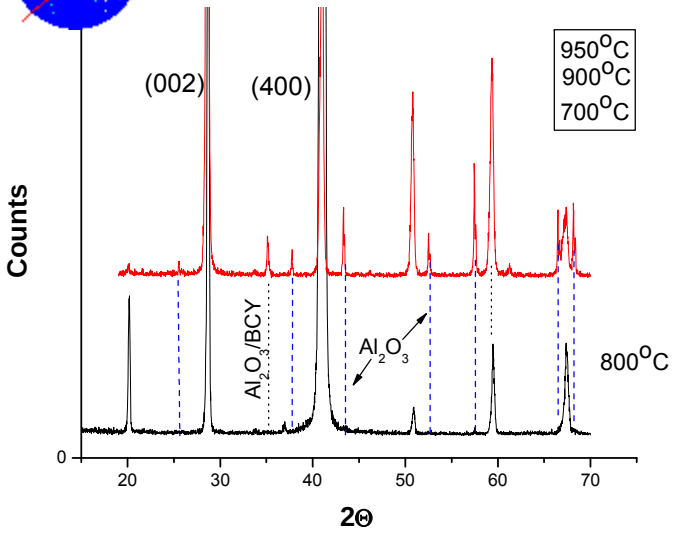

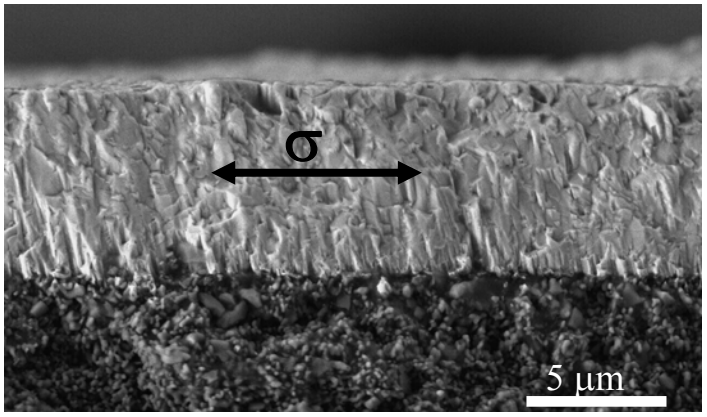

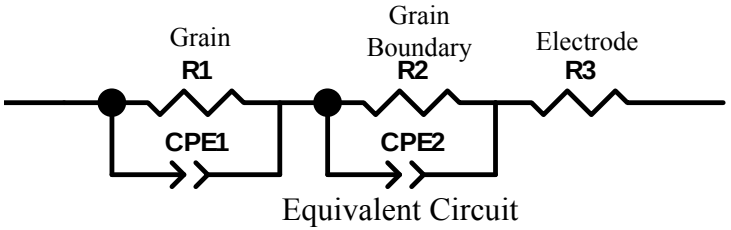

Equivalent Circuit

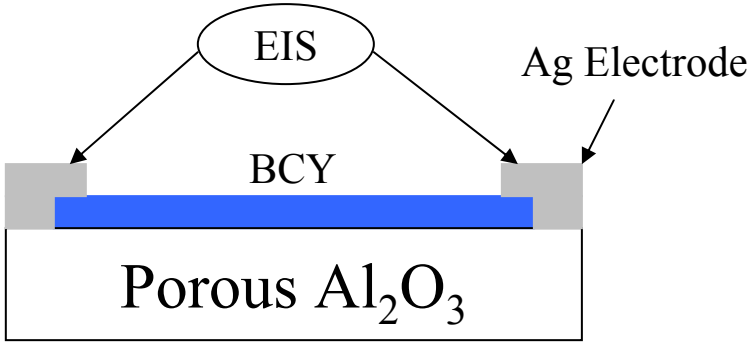

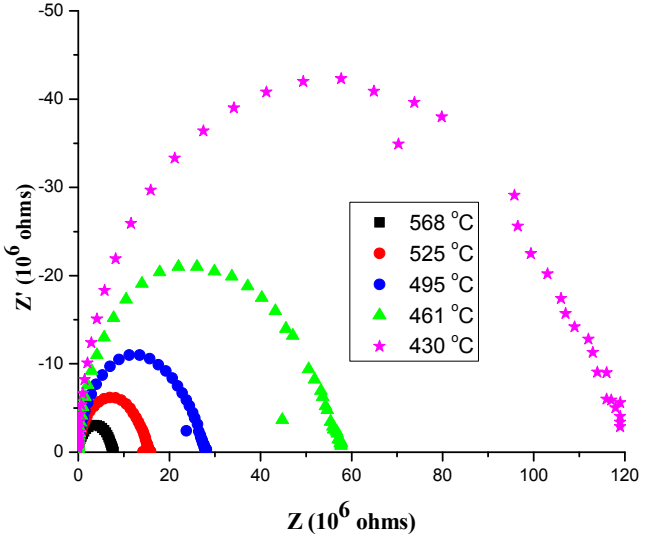

Solartron 1260/1296 0.1 – 1MHz 100 °C – 950 °C
Air – 25 °C Zplot/Zview Software

Microstructure Characterization

$BaCe_{0.85}Y_{0.15}O_{3-\delta}$ Film

800 °C Deposition Temperature

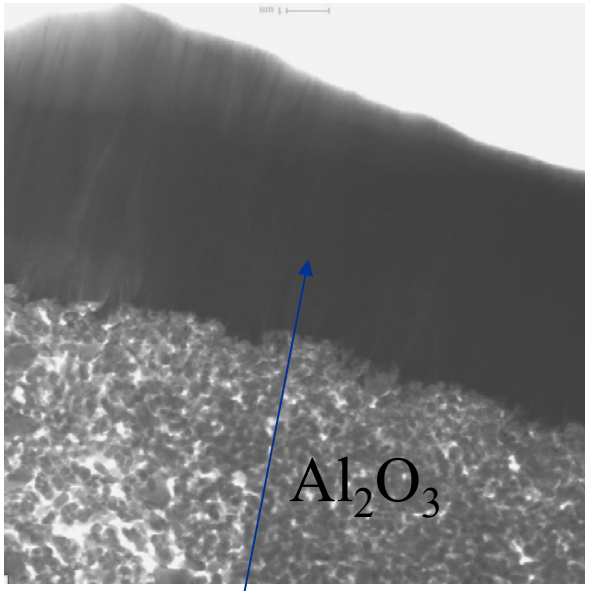

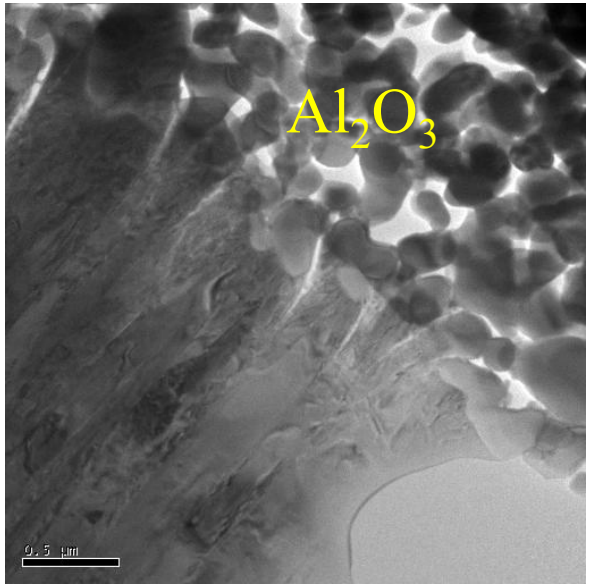

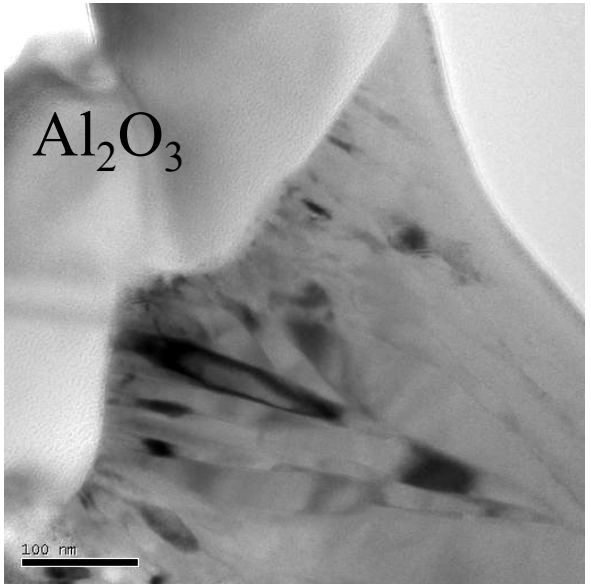

Dense films fabricated at 600-950 °C

No inclusions from PLD

Al_2O_3 particles determine column width.

Dense films form by impinging column growth.

No long range defects

Numerous BCY nano-crystals nucleate at the Al_2O_3 particle surface.

Thin amorphous layer

Interface Characterization

$BaCe_{0.85}Y_{0.15}O_{3-\delta}$ Film

950 °C Deposition Temperature

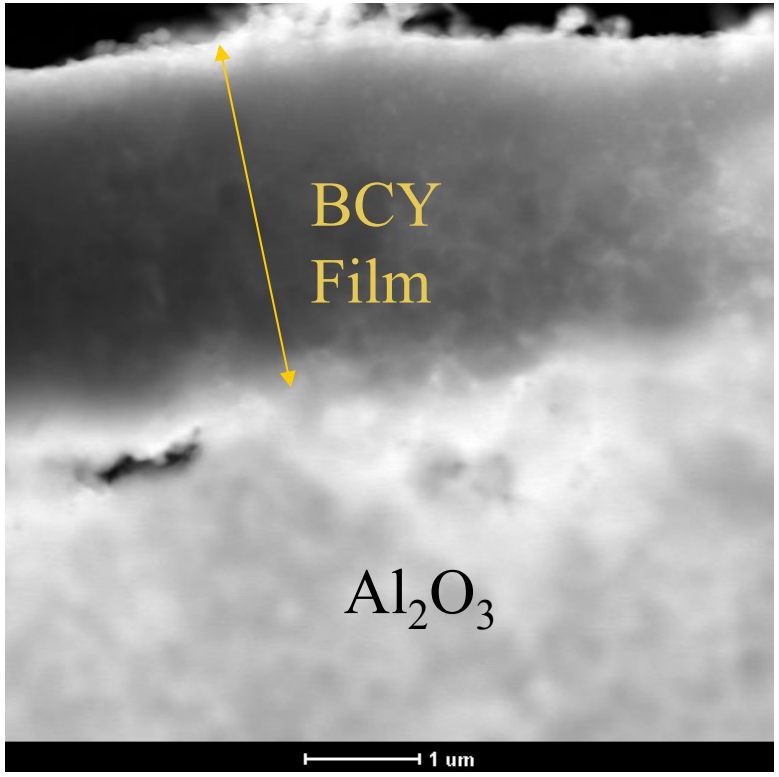

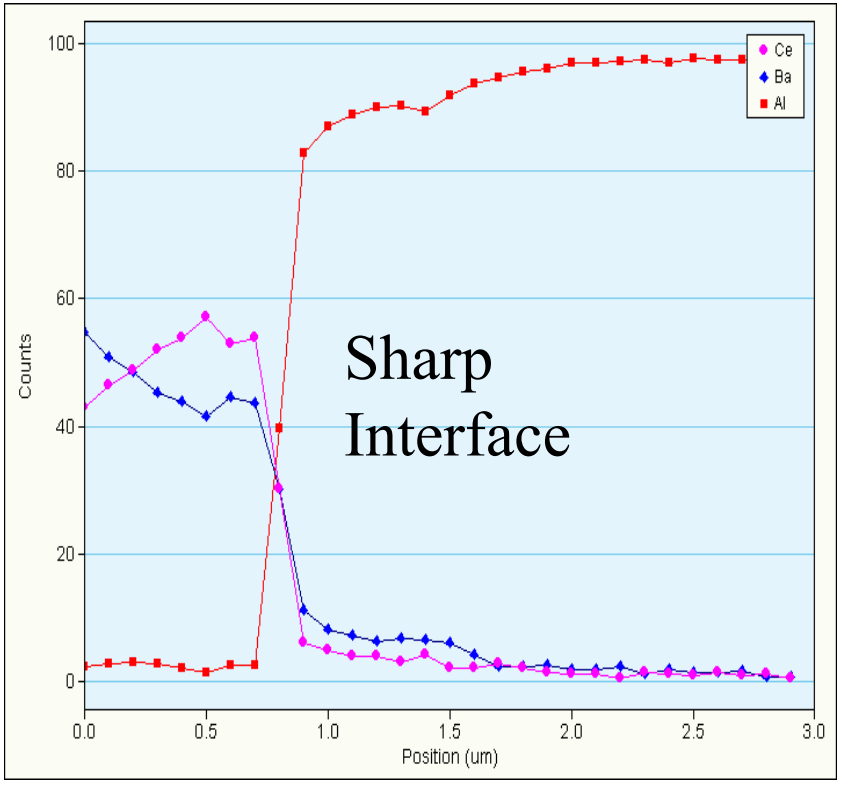

Total Conductivity
Porous Al_2O_3 Substrates

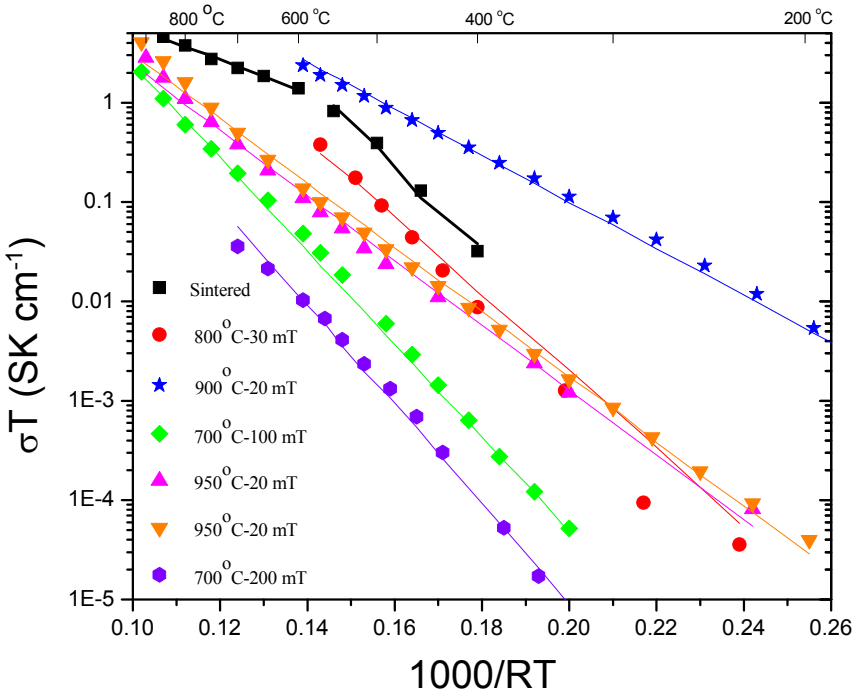

$$\sigma \cdot T = A \cdot \exp(-Q/RT)$$

Activation Energy

	Temp. (°C)	Q (KJ/mol)	Film Thickness (μm)
$BaCe_{0.85}Y_{0.15}O_3$ Sintered	600 - 850 400 - 550	38.6 100.3	
950 °C/30 mT	200 - 900	74.8	3.6
950 °C/30 mT	200 - 900	75.4	3.2
900 °C/30 mT	200 - 600	54.1	4.8
800 °C/30 mT	200 - 600	98.1	3.6
700 °C/100 mT	350 - 900	115.6	1.7
700 °C/200 mT	350 - 700	108.2	4.1

Protonic Conduction – 48 – 100 KJ/mol

Conduction exhibits large dependence on process conditions.

Porous $BaZrO_3$ Substrates

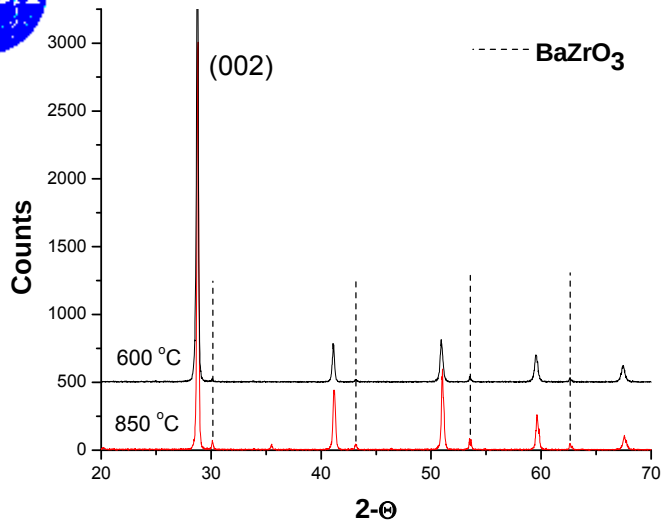

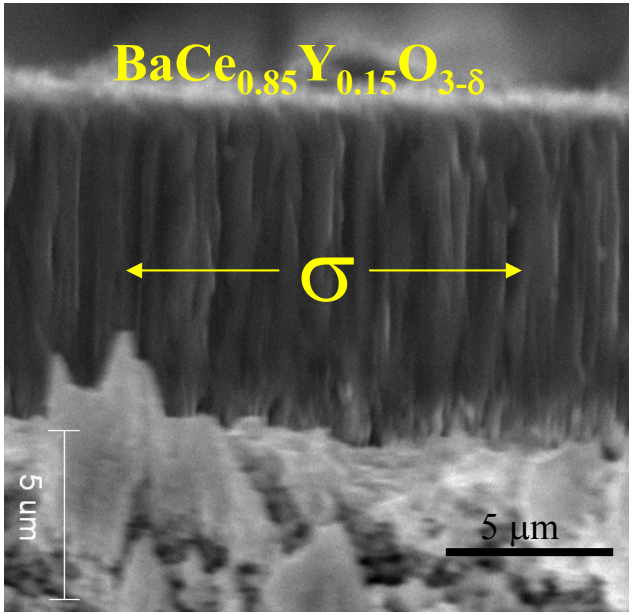

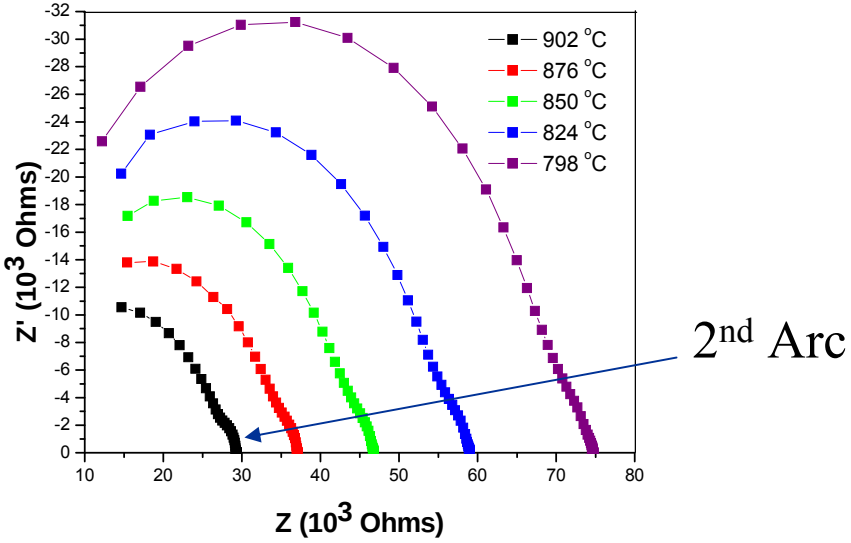

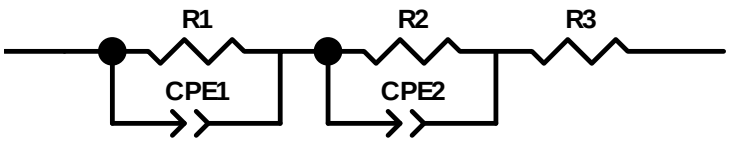

Equivalent Circuit

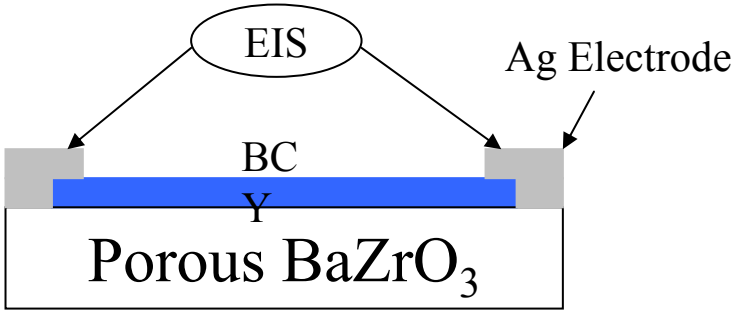

Solartron 1260/1296 0.1 – 1MHz 100 °C – 950 °C
Air, 5%H_2/N_2 Zplot/Zview Software

Microstructure Characterization

$BaCe_{0.85}Y_{0.15}O_{3-\delta}$ Film

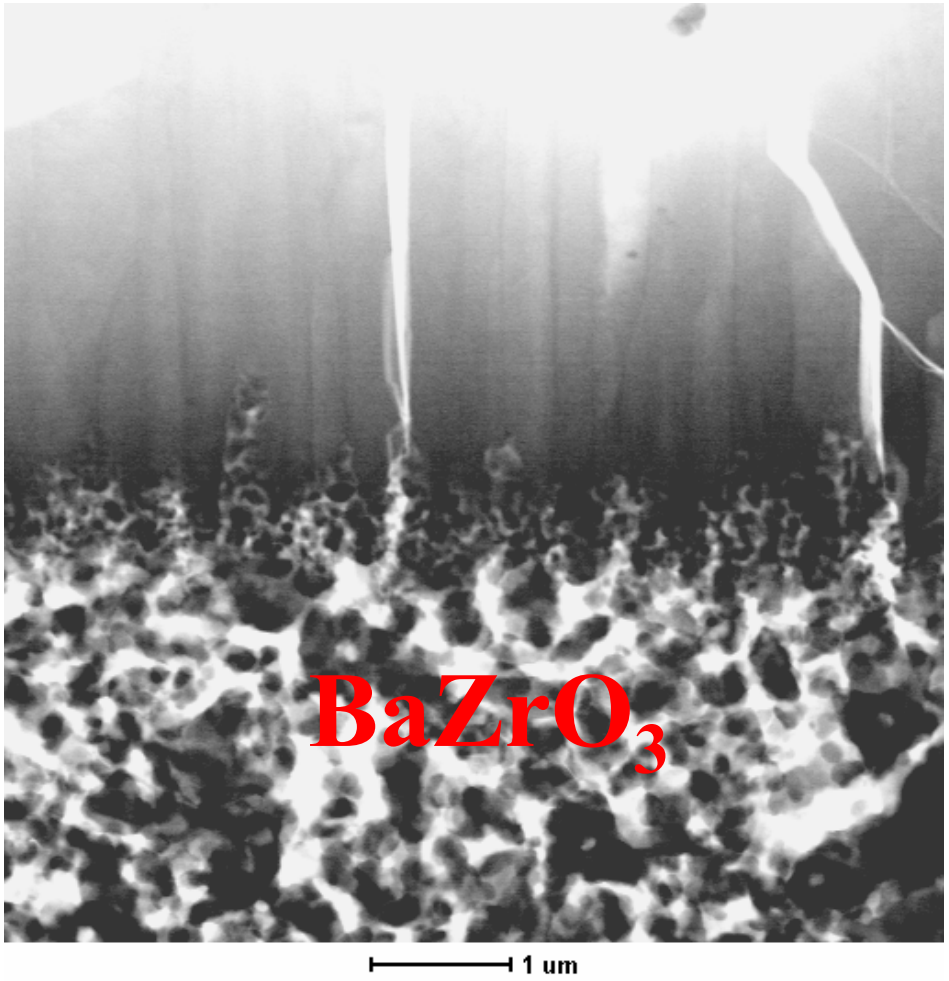

- Columnar grains
- No particle inclusions from PLD
- Low defects
- No long range ordering

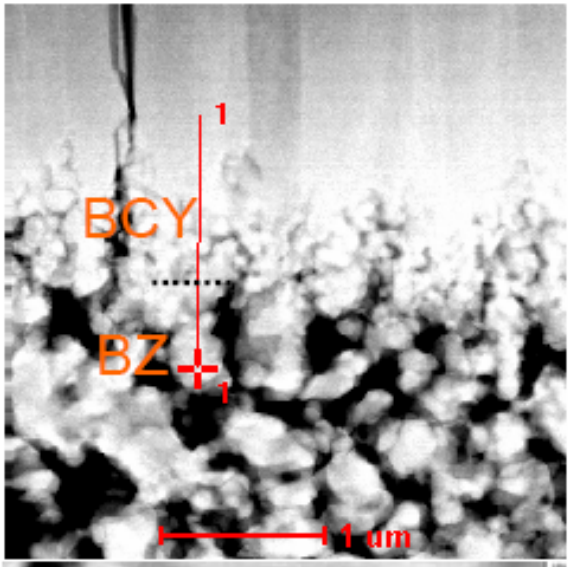
1
BCY
BZ
1
1 um

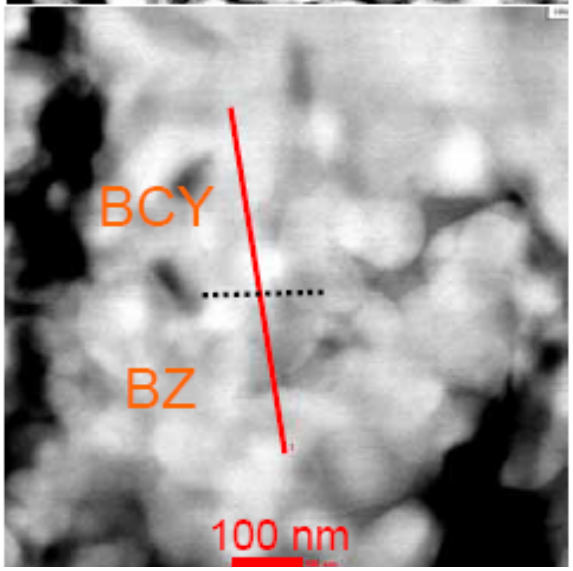
BCY
BZ
100 nm

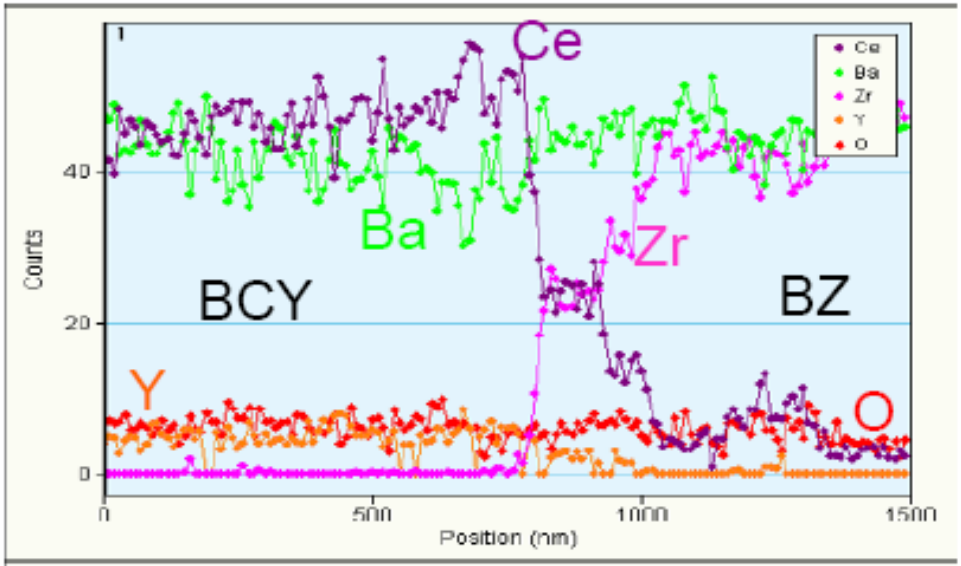
1
Ce
Ba
Zr
Y
O
BCY
BZ
Counts
Position (nm)
0
20
40
500
1000
1500

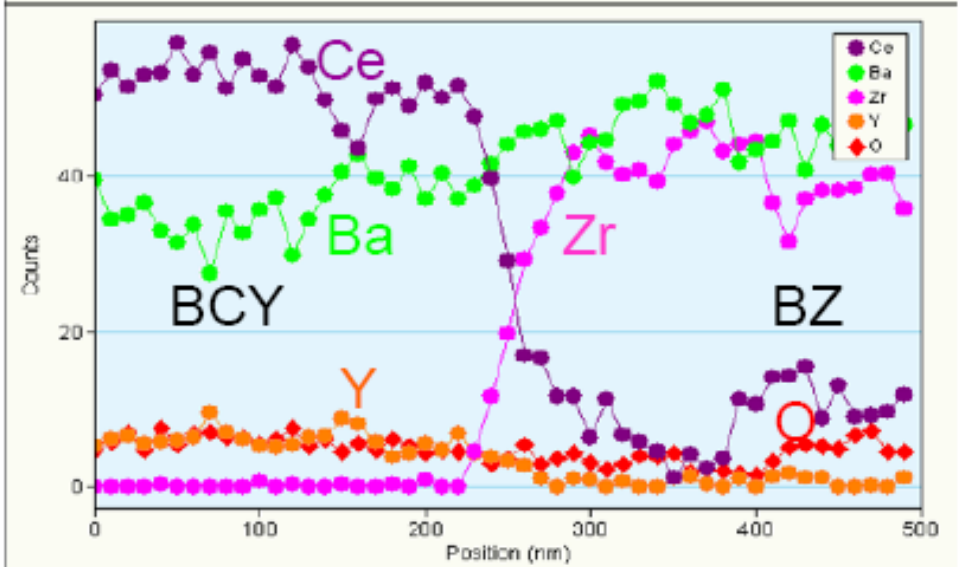
Ce
Ba
Zr
Y
O
BCY
BZ
Counts
Position (nm)
0
20
40
100
200
300
400
500

Growth Segregation

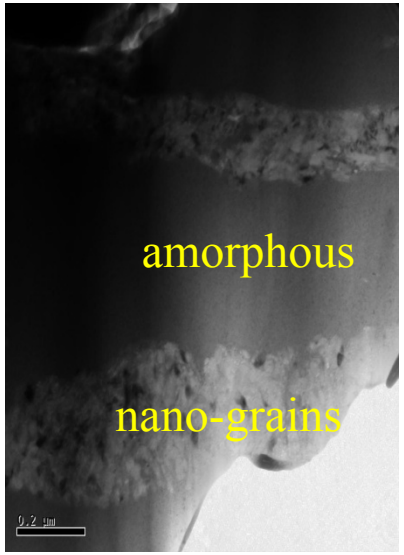

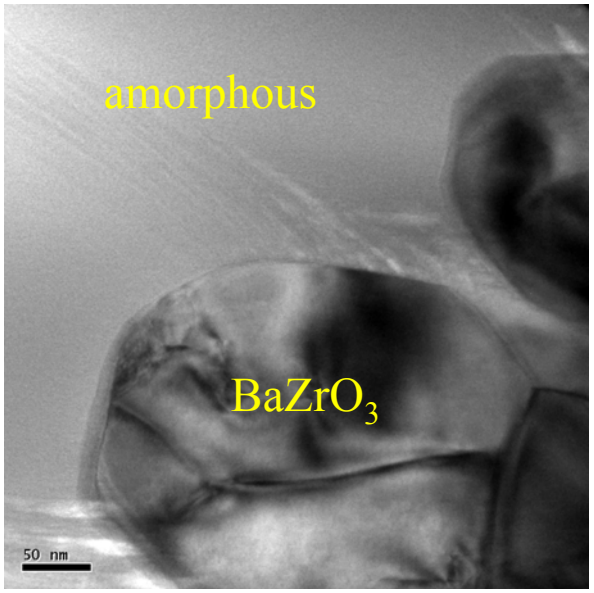

Small domains 2 nm visible
3.1 Ang … make the continuous circle

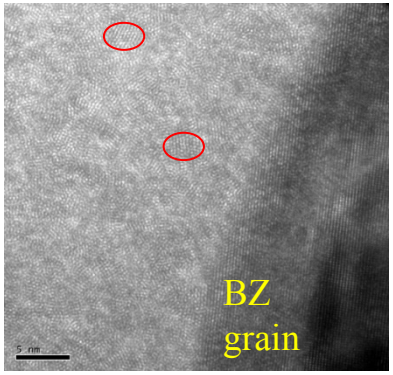

~20 nm grains

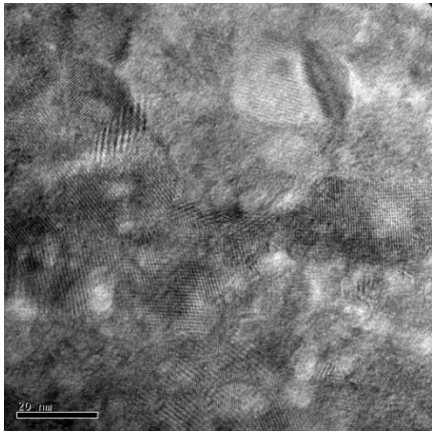

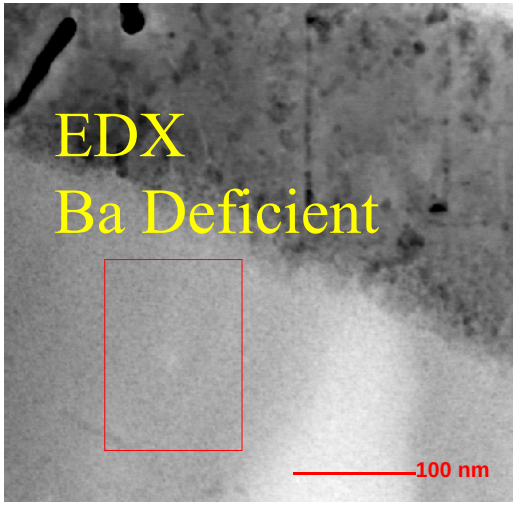

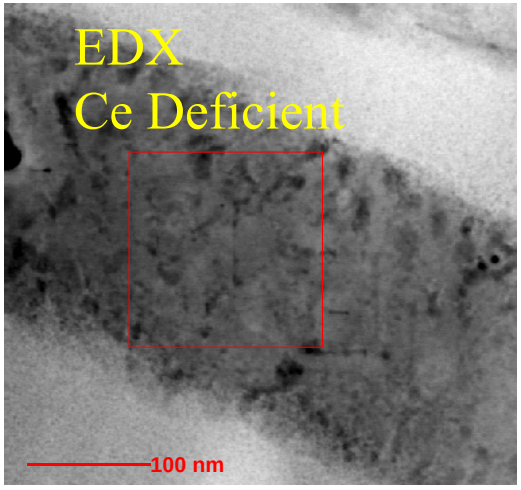

Total Conductivity
Porous $BaZrO_3$ Substrates

$BaCe_{0.85}Y_{0.15}O_{3-\delta}$

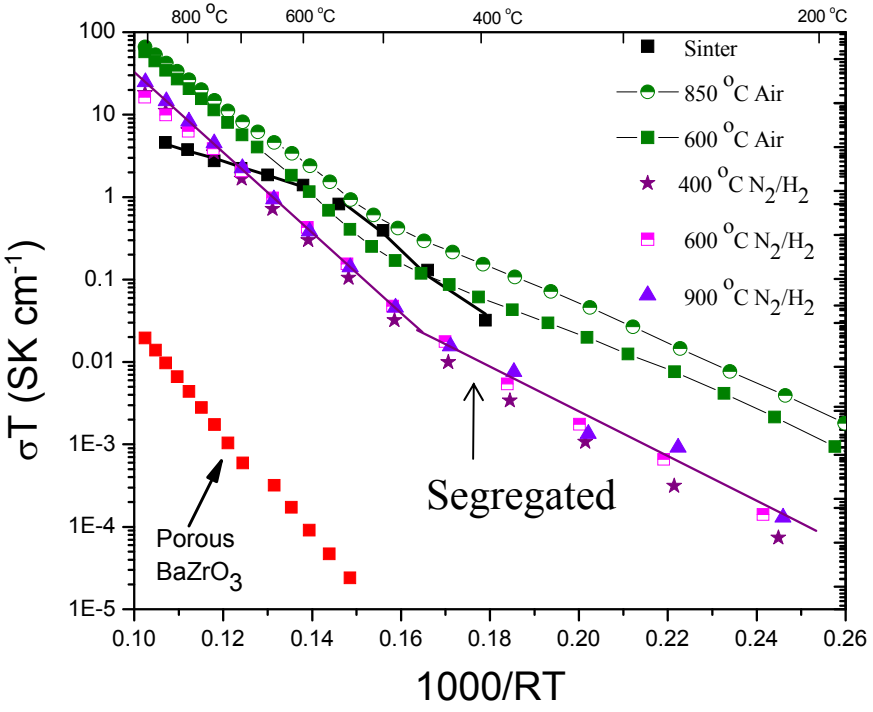

$\sigma \cdot T = A \cdot \exp(-Q/RT)$

Activation Energy

	Temp. (°C)	Q (KJ/mol)	Film Thickness (μm)
$BaCe_{0.85}Y_{0.15}O_3$ Sintered	600 - 850 400 - 550	38.6 100.3	
850 °C/20 mT	550 – 900 100 - 550	89.7 56.8	9.4
600 °C/30 mT	550 – 900 100 - 550	106.7 55.2	5.9
400 °C/20 mT	550 – 900 100 - 550	111.5 48.1	3.8
600 °C/20 mT	550 – 900 100 - 550	102.9 45.7	1.0
900 °C/20 mT	550 – 900 100 - 550	112.2 62.5	3.1

- σ less dependent upon process conditions
- Conduction change at T >550 °C

Summary

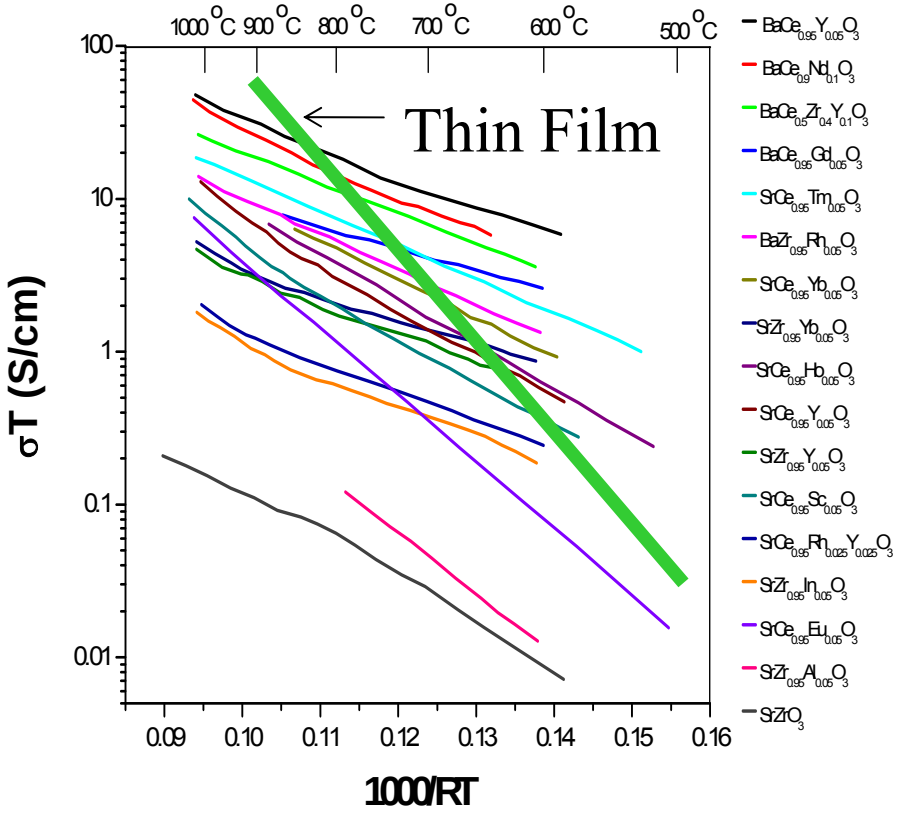

- Directionally solidified samples exhibit similar ionic conduction to reported data for sintered samples.
- Directional solidification produces nano-sized structural defects. Influence of defects on proton mobility remains unknown.
- Directional solidification can produced unique microstructures that can not be achieved by solid state sintering.
- Dense protonic films can be fabricated on porous substrates by PLD in the temperature range of 600-950 °C.
- Columnar growth morphologies are observed at temperature <950 °C. Process dependent oriented crystal growth occurs among the [100] and [001] directions.
- Matching crystal symmetry between substrate & film is essential to maximize protonic conduction.